Journal of Macromolecular Science, Part A
Publication details, including instructions for authors and subscription information:
http://www.informaworld.com/smpp/title~content=t713597274

Copolymerization of Vinyl Chloride and Sulfur Dioxide. III. Evaluation of the Copolymerization Mechanism

R. E. Cais[ab]; D. J. T. Hill[a]; J. H. O'donnell[a]
[a] Chemistry Department, University of Queensland, Queensland, Australia [b] Bell Laboratories, Murray Hill, New Jersey

To cite this Article Cais, R. E. , Hill, D. J. T. and O'donnell, J. H.(1982) 'Copolymerization of Vinyl Chloride and Sulfur Dioxide. III. Evaluation of the Copolymerization Mechanism', Journal of Macromolecular Science, Part A, 17: 9, 1437 — 1467
To link to this Article: DOI: 10.1080/00222338208074408
URL: http://dx.doi.org/10.1080/00222338208074408

J. MACROMOL. SCI.–CHEM., A17(9), pp. 1437-1467 (1982)

Copolymerization of Vinyl Chloride and Sulfur Dioxide. III. Evaluation of the Copolymerization Mechanism

R. E. CAIS,* D. J. T. HILL, and J. H. O'DONNELL†

Chemistry Department
University of Queensland
Brisbane 4067, Queensland, Australia

ABSTRACT

The mechanism of copolymerization of vinyl chloride (V) with sulfur dioxide (S) to form a variable composition polysulfone with average V:S molar ratio $\bar{n} \geq 1$ is examined. The copolymerization deviates from Lewis-Mayo behavior above -78° C. Alternative models for propagation involving (1) penultimate and pen-penultimate unit effects, (2) complex participation, and (3) depropagation are considered quantitatively by comparison of calculated and experimental copolymer/comonomer composition relationships and comonomer sequence distributions. Our theoretical modeling of the copolymerization shows that it is difficult to discriminate convincingly between alternative mechanisms. The penultimate and pen-penultimate effect models can account for the copolymer compositions, but not for the dilution effects which were observed provided the diluent is truly inert. The complex participation model can account for experimental behavior from -78 to -18° C by the assumption of addition of SV complexes, but it becomes rapidly less satisfactory at higher temperatures. Depropagation

*Present address: Bell Laboratories, Murray Hill, New Jersey, 07974.

†To whom correspondence should be addressed.

is the only model which can account for the compositions and dilution effects above 0°C. Progressive depropagation, with increasing temperature, of chains ending in the triad sequences ~SVS•, ~VVS•, and ~VSV• can explain the observed behavior over the entire comonomer composition and temperature range, but involvement of comonomer complexes in the propagation reactions is highly likely below 0°C.

INTRODUCTION

In this paper we consider the mechanism of copolymerization of vinyl chloride (V) with sulfur dioxide (S). The copolymerization can be initiated by γ-irradiation or by some chemical initiators, and proceeds via a free radical, chain-growth reaction in the liquid phase between -90 and +55°C to produce a copolymer of variable composition. The copolymer has a V:S molar ratio $\bar{n}$ which increases with polymerization temperature T_p and vinyl chloride content of the comonomer feed [1].

Copolymerization rates and the composition of poly(vinyl chloride sulfone)s prepared by γ-irradiation at -78 and 20°C have been reported by Schneider et al. [2] and also by Suzuki et al. [3]. Schneider et al. [2] proposed that the mechanism suggested by Barb [4] for the formation of poly(styrene sulfone), involving participation of a 1:1 comonomer complex, would explain their results. No depropagation or penultimate effects were considered and SO_2 was assumed to be incorporated only via the 1:1 complex and only in the direction of SV. They did not test this model quantitatively.

Suzuki et al. [3] suggested a Lewis-Mayo model with one reactivity ratio equal to zero. Unimolecular termination was assumed to explain the observed dose-rate exponent of unity, and a complex kinetic expression was derived which was claimed to explain the results for polymerization rates.

We have previously [5] investigated complex formation between vinyl chloride and SO_2; two complexes of composition VS and VS_2 were shown to form with significant equilibrium constants. Although they may well be involved in the copolymerization at low temperatures, measurements of the number fractions of SVS sequences in copolymers prepared from -78 to 0°C and of composition relationships above 0°C suggested that depropagation reactions were involved. We outlined the possible involvement of successive depropagation reactions of three different terminal triads in a preliminary publication [6]. Recently, Matsuda and Thoi [7] have reported measurements on the copolymerization at $T_p \geq 0$°C and considered a mechanism involving an unusual depropagation step.

In order to discriminate between various possible copolymerization mechanisms, adequate experimental information is required. This may include (1) average copolymer composition versus comonomer composition relationships; (2) comonomer sequence distributions in the copolymer; (3) effects of dilution by a third (inert) component on (1) and (2); (4) effects of the polymerization temperature on (1), (2), and (3); (5) copolymerization rate as a function of comonomer composition and copolymerization temperature; and (6) copolymer molecular weights. The evaluation of possible polymerization mechanisms may be via qualitative argument [2, 7], consideration of equations for limiting situations [6], or comparison of calculated and experimental values of any of the types of information above.

In the previous paper we reported measurements of average copolymer compositions and copolymerization rates as functions of comonomer composition and temperature over the entire liquid-phase copolymerization range, together with dilution effects on the copolymer composition and the comonomer sequence distributions. A study of the ^{1}H NMR spectra of poly(vinyl chloride sulfone)s [8] had provided information on comonomer sequence distributions for $T_p \leq 0°C$.

In the present paper we consider the applicability of alternative models for the copolymerization mechanism which are tested by comparing quantitative predictions of (1) copolymer composition versus comonomer composition relationships and (2) comonomer sequence distributions, using appropriate values for reactivity ratios and equilibrium constants, with experimental results.

RESULTS AND DISCUSSION

Comonomer Sequence Distributions from ^{1}H NMR Spectra

The determination of average copolymer compositions from the areas of diad resonances in the ^{1}H NMR spectra are discussed in the previous paper [1]. Thus, $\bar{n} = 1 + A_{VV}(CH_2)/2A_{VS}(CH)$, where A_{VV} and A_{VS} are the areas of the VV and VS diad resonances, respectively. The comonomer sequence distributions were also determined from the ^{1}H NMR spectra [8]. The most accurate results were obtained for copolymers prepared from vinyl chloride-β,β-d_2, (CD_2=CHCl), which showed a good separation of the SVS and SVVS resonances from the α-sulfonyl methine proton in SV diads.

The number-fraction of SVS sequences N(1) in a particular poly(vinyl chloride sulfone) is given by the area (A) of resonances due to protons in SVS sequences relative to the total area for all SV_nS

sequences, adjusted to the same number of protons for each value of n. N(1) should be equal to the probability p(1) that a randomly chosen sequence of V units has n = 1, calculated from the proposed propagation mechanism. This is not the probability of finding a SVS triad, but is related to it according to

$$N(1) = p(SVS)/p(S) \tag{1}$$

We have defined the sequence probabilities over the state space of all SV_nS sequences with n = 1 to ∞. This definition is the most suitable one since there are no SS sequences in poly(vinyl chloride sulfone). The average composition of the copolymer can also be calculated from the sequence distribution, since

$$\bar{n} = \sum_{n=1}^{\infty} nN(n) \tag{2}$$

Thus, for copolymers with $\bar{n} \leq 2$ (which we have shown to have negligible proportions of SVVVS sequences)

$$\bar{n} = N(1) + 2N(2) = 2.0 - N(1) \tag{3}$$

since N(1) + N(2) = 1.0 when N(≥ 3) = 0.

When dehydrochlorination to ethene units E had occurred, a corrected value for A(SVS) was used, equal to $A(SVS)_{obs}$ + A(SES), since only SVS sequences lost HCl under normal conditions.

The values of N(1) and N(2) determined from the ^1H NMR spectra of a range of comonomer compositions and copolymerization temperatures are shown in Table 1. The agreement between values of $\bar{n}$ calculated from (a) sequence distributions and (b) areas of diad resonances is good, supporting the ^1H NMR assignments.

It was not possible to discriminate between the sequences SVVS, SVVVS, etc. from the ^1H NMR spectra, except for the deuterated polymer with $\bar{n} \approx 2$; nor could they be distinguished in the ^{13}C NMR spectra [9]. However, both ^1H and ^{13}C NMR showed conclusively that N(1) ≈ 0.0 for all copolymers prepared above 0°C.

Copolymerization Models

Pen-Penultimate, Penultimate, and Terminal Models

The pen-penultimate effect model was considered first, since it could be reduced to the penultimate and terminal (Lewis-Mayo) models by appropriate simplifications. The reaction scheme with complete generality is shown in Table 2 and the expressions for the copolymer

TABLE 1. Monomer Sequence Distributions in Poly(vinyl Chloride Sulfone) Determined from ^{1}H NMR Spectra

Copolymerization temperature (°C)	$(\bar{x}_V)_m$	N(1)	N(2)	$\bar{n}^a$	$\bar{n}^b$
-78	0.22	0.93	0.07	1.07	1.03
	0.33	0.89	0.11	1.11	1.13
	0.42	0.90	0.10	1.10	1.04
	0.62	0.87	0.13	1.13	1.10
	0.80	0.78	0.22	1.22	1.20
-45	0.21	0.83	0.17	1.17	1.20
	0.42	0.68	0.32	1.32	1.40
	0.44	0.63	0.37	1.37	1.40
	0.62	0.63	0.37	1.37	1.50
	0.81	0.34	0.66	1.66	1.60
-18	0.22	0.38	0.62	1.62	1.60
	0.42	0.28	0.72	1.72	1.80
	0.62	0.13	0.87	1.87	1.90
	0.80	0.01	0.99	1.99	2.00
0	0.40	0.04	0.96	1.96	2.00

[a]Calculated from diad resonance areas in ^{1}H NMR spectra.
[b]Calculated from N(1) and N(2) according to Eq. (3).

composition and the comonomer sequence distributions are given in the Appendix. For the copolymerization of vinyl chloride and sulfur dioxide, the absence of –SS– sequences allows the simplifications which are shown.

The expressions for the penultimate-effect model are readily derived from those for the pen-penultimate model by equating the transition probabilities which differ only by a pen-penultimate effect, as shown in the Appendix. Similarly, the terminal model can be derived from the penultimate model by equating those transition probabilities which differ only by a penultimate effect.

Complex Participation Model

The general propagation scheme for this model is given in Table 3.

TABLE 2. Pen-Penultimate Effect Propagation Mechanism Showing Conditional Probabilities and Reactivity Ratios

Initial state			Final state		Conditional transition probability		Reactivity ratios		
Binary	Decimal (J)	Add	Binary	Decimal (K)	P(J, K)	Rate constant	Binary	Decimal	V + S
000	0	0	000	0	P_{00}	k_{0000}			
000	0	1	001	1	P_{01}	$\overline{k_{0001}}$	$= r_{000}$	$= r_0$	$= 0$
001	1	0	010	2	P_{12}	k_{0011}			
001	1	1	011	3	P_{13}	$\overline{k_{0010}}$	$= r_{001}$	$= r_1$	
010	2	0	100	4	P_{24}	k_{0100}			
010	2	1	101	5	P_{25}	$\overline{k_{0101}}$	$= r_{010}$	$= r_2$	$= 0$
011	3	0	110	6	P_{36}	$k_{01\,11}$			
011	3	1	111	7	P_{37}	$\overline{k_{0110}}$	$= r_{011}$	$= r_3$	
100	4	0	000	0	P_{40}	k_{1000}			
100	4	1	001	1	P_{41}	$\overline{k_{1001}}$	$= r_{100}$	$= r_4$	$= 0$
101	5	0	010	2	P_{52}	k_{1011}			
101	5	1	011	3	P_{53}	$\overline{k_{1010}}$	$= r_{101}$	$= r_5$	
110	6	0	100	4	P_{64}	$k_{11\,00}$			
110	6	1	101	5	P_{65}	$\overline{k_{11\,01}}$	$= r_{110}$	$= r_6$	$= 0$
111	7	0	110	6	P_{76}	k_{1111}			
111	7	1	111	7	P_{77}	$\overline{k_{1110}}$	$= r_{111}$	$= r_7$	

TABLE 3. Propagation Mechanism for the Complex Participation Model

Initial state	Add	Final state	Rate constant	Transition probability
0	0	0	k_{00}	P_{00}
0	1	1	k_{01}	P_{01}
0	$\overline{10}$	0	$k_{0\overline{10}}$	$P_{0\overline{10}}$
0	$\overline{01}$	1	$k_{0\overline{01}}$	$P_{0\overline{01}}$
1	0	0	k_{10}	P_{10}
1	1	1	k_{11}	P_{11}
1	$\overline{10}$	0	$k_{1\overline{10}}$	$P_{1\overline{10}}$
1	$\overline{01}$	1	$k_{1\overline{01}}$	$P_{1\overline{01}}$

The reactivity ratios for copolymerization of vinyl chloride and SO_2 are reduced to

$$r_1 = k_{11}/k_{10}, \qquad s_0 = k_{0\overline{10}}/k_{01}$$

$$p_1 = k_{1\overline{10}}/k_{1\overline{01}}, \qquad s_1 = k_{1\overline{01}}/k_{10}$$

We have solved [10] this scheme using a kinetic-probabilistic method to obtain the expressions for copolymer composition and sequence distributions. Litt and Seiner [11] had previously obtained an equation for the copolymer composition and evaluated it when –OO– sequences were not formed, with severe limitations.

Depropagation Model

The proposed reaction scheme, which may be regarded as a special case of the triad model of Howell et al. [12], is given in Table 4. The rate constants for propagation and depropagation can be related by reactivity ratios and equilibrium constants according to

$$r_1 = k_{111}/k_{110}, \qquad r_2 = k_{011}/k_{010}$$

$$s_1 = k_{010}/k_{101}, \qquad s_2 = k_{110}/k_{101}$$

We have considered the reversibility of three propagation reactions:

TABLE 4. Propagation Mechanism for the Depropagation Model.[a] (The decimal states used as suffixes in the transition probabilities correspond to those used for the penultimate and pen-penultimate effect models.)

Initial state	Add	Rate constant	Final state	State transition probability
11	+0	k_{110}	110	P_{36}
	+1	k_{111}	11	P_{33}
01	+0	k_{010}	010	P_{12}
	+1	k_{011}	11	P_{13}
	-1	d_{101}	10	D_1
010	-0	d_{010}	01	D_{21}
	+1	k_{101}	01	P_{21}
110	-0	d_{110}	11	D_{63}
	+1	k_{101}	01	P_{61}

[a] States: Binary 01 11 010 110
Decimal 1 3 2 6

$$\sim\sim SM^{\bullet} + S \underset{d_{010}}{\overset{k_{010}}{\rightleftharpoons}} \sim\sim SMS^{\bullet}, \qquad K_p \text{ (penultimate)} = k_{010}/d_{010}$$

$$\sim\sim MS^{\bullet} + M \underset{d_{101}}{\overset{k_{101}}{\rightleftharpoons}} \sim\sim MSM^{\bullet}, \qquad K_V \text{ (vinyl chloride)} = k_{101}/d_{101}$$

$$\sim\sim MM^{\bullet} + S \underset{d_{110}}{\overset{k_{110}}{\rightleftharpoons}} \sim\sim MMS^{\bullet}, \qquad K_T \text{ (terminal)} = k_{110}/d_{110}$$

We will show that the copolymerization of vinyl chloride with sulfur dioxide can be described by this depropagation model with K_p decreasing below 0°C and either K_T or K_V decreasing at higher temperatures. We do not distinguish between the rate of addition of V to ~S· with different pen-penultimate units, i.e., we assume $k_{1101} = k_{0101}$. Also, if there is no kinetic, penultimate effect on the rate of addition of V and S, then $r_1 = r_2$ and $s_1 = s_2$.

Defining the state-transition probabilities on a kinetic basis:

$$P_{JK} = [\text{rate}(J \rightarrow K)] / [\sum_K (\text{rate } J \rightarrow K)]$$

the following transition probabilities are obtained:

$$P_{33} = (r_1 f_1)/(r_1 f_1 + f_0), \qquad P_{12} = (K_V s_1 f_0)/(1/W + K_V s_1\{r_2 f_1 + f_0\})$$

$$D_1 = 1/(1 + K_V s_1 W\{r_2 f_1 + f_0\}), \qquad D_{21} = s_1/(s_1 + K_p f_1 W)$$

$$D_{63} = s_2/(s_2 + K_T f_1 W)$$

and the stochastic relationships are

$$P_{36} + P_{33} = 1, \qquad P_{12} + P_{13} + D_1 = 1$$

$$D_{21} + P_{21} = 1, \qquad D_{63} + P_{61} = 1$$

A general analytical solution for the composition equation was obtained by Lauritzen et al. [13] and also by O'Driscoll et al. [14]. However, we have chosen a Monte-Carlo simulation procedure in order to provide a direct visualization of the copolymerization and generate the copolymer composition, sequence distribution, degree of copolymerization, and overall propagation rate, since we know far too few parameters for an analytical approach. Figure 1 shows a partial schematic flow chart of the computer program for the simulation.

Comparison of Calculated and Experimental Results

The experimental results [1] for copolymer compositions and copolymerization rates suggest that the temperature range can be

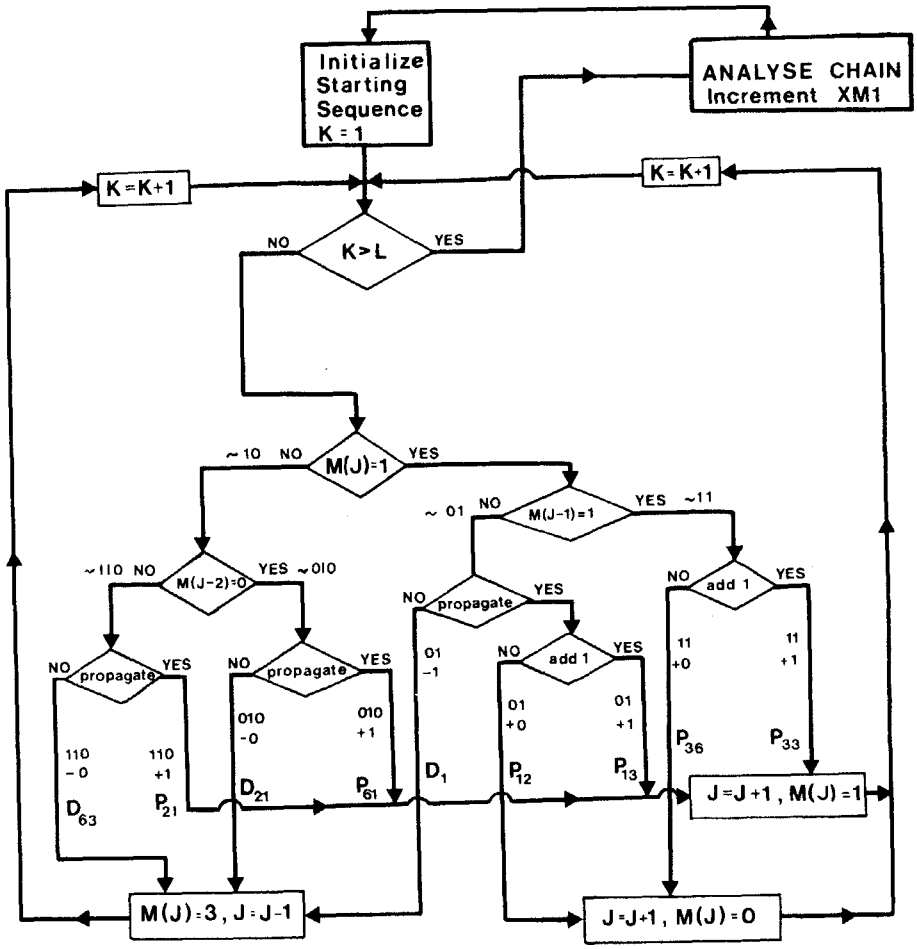

FIG. 1. Schematic, partial flow chart for simulation of copolymer chains using the depropagation model shown in Table 4. K = counter for number of trials executed (L is the chosen limit). J = index of current chain position. M(J) = monomer unit at current index = 0 (S), 1 (V), or 3 (error detection). The decisions (i) to propagate or depropagate, and (ii) the addition of 0 or 1 are made on the basis of the test between the relevant state transition probability $P_{I,J}$ or $D_{I,J}$ and a computer-generated random number. XM1 = mole fraction of V in comonomer feed.

conveniently divided into two regions; I: -95 to 0° C, and II: 0 to 55° C, for comparison with calculations based on the various models.

Lewis-Mayo Model

This model is characterized by one reactivity ratio r_1 for V-S copolymerization since $r_0 = 0$. Satisfactory agreement between experimental and computed composition curves and sequence distributions is obtained only for $T_p \leq -78°$ C, with $r_1 = 0.04$-0.08. This value of r_1 indicates that the cross-propagation step $\sim V^{\bullet} + S$ is 10-25 times faster than the homopropagation step $\sim V^{\bullet} + V$ at these temperatures. This is not unreasonable in view of the highly electrophilic nature of S compared with V.

The model does not predict any change in copolymer composition or sequence distribution with a change in total comonomer concentration which is effectively in accord with the experimental results at -78° C, but not at higher temperatures. The model does not describe the composition behavior above -78° C as it always gives symmetrical composition curves between (0.5, 0.5) and (1.0, 1.0). Thus the claim by Suzuki et al. [3] that the copolymerization may be described by the Lewis-Mayo model at room temperature can be refuted.

Penultimate-Effect Model

This model is characterized by two reactivity ratios, $r_1 = k_{001}/k_{010}$ and $r_3 = k_{111}/k_{110}$, for V-S copolymerization. Increasing r_1 (retardation of $\sim SV^{\bullet} + S$) with r_3 small (cf. 0.08 at -78 C for the Lewis-Mayo model) favors the formation of SVVS sequences. Figure 2 shows that the composition data at -18 and 0° C can be explained by the penultimate model with the reactivity ratios shown in Table 5, but that the apparent sigmoidal relationship at -45° C cannot be matched satisfactorily. The computed sequence distributions also agree well with the experimental values as shown in Fig. 3. With $r_1 \gg 1$ the effect of r_3 is similar to Lewis-Mayo behavior with one comonomer a dimer (VV) and all calculated composition curves are concave below and convex above the line joining $(x_V)_m$, $(x_V)_p = 0.0, 0.67$ to $1.0, 1.0$. Therefore, the curves differ from the experimental relationships for $T_p > 0°$ C. The model can also be rejected above 0° C because there are no terms in the equations which involve individual monomer concentrations and hence it cannot predict any dilution effect on composition, which is quite pronounced. Similarly, it cannot account for the observed change in sequence distribution at -18° C (N(010) reduced to zero and $\bar{n}$ increased).

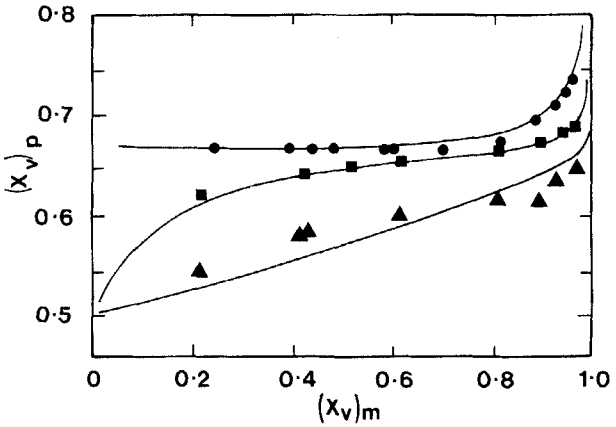

FIG. 2. Copolymer versus comonomer composition relationships calculated for the penultimate-effect model at -45, -18, and 0°C from the reactivity ratios shown in Table 5. Experimental values: (▲) -45°C; (■) -18°C, (●) 0°C.

TABLE 5. Reactivity Ratios for Copolymerization in the Temperature Range -45 to 0°C for the Penultimate Model

Temperature (°C)	r_1	r_3
-45	0.5	0.001
-18	5.0	0.01
0	1000	0.04

Pen-Penultimate-Effect Model

This model can give a good simulation of the experimental comonomer copolymer composition relationships at 30 and 46°C as shown in Fig. 4 using the reactivity ratios given in Table 6. Since sequences SV_nS with $n > 2$ could not be discriminated in the NMR spectra of copolymers with $n \geq 2$, the computed distributions cannot be tested. Although the model will match the composition data, it cannot predict the marked dilution effect which was observed and for this reason must be considered inappropriate.

Complex-Participation Model

We have evaluated the applicability of the complex participation model to the copolymerization between -78 and -18°C by utilizing the

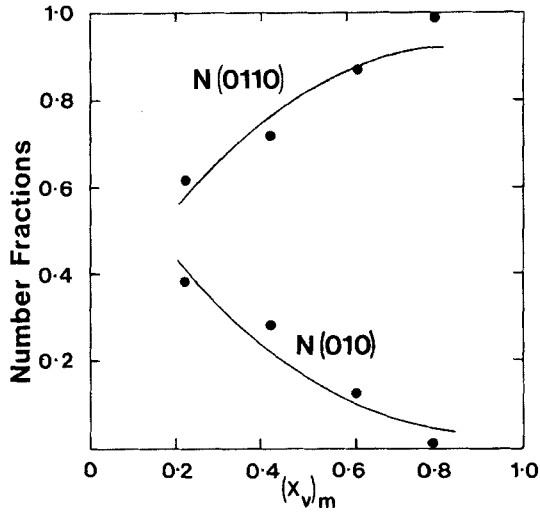

FIG. 3. Calculated (full lines) and experimental sequence distributions for the penultimate-effect model at ~18° C.

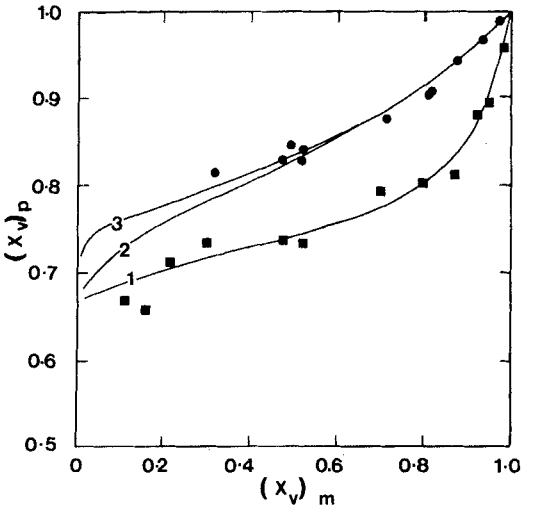

FIG. 4. Calculated (full lines) and experimental copolymer versus comonomer composition relationships calculated for the pen-penultimate-effect model at 30 and 46° C from the reactivity ratios shown in Table 6. Experimental values: (■) 30° C; (●) 46° C.

TABLE 6. Reactivity Ratios for Copolymerization at 30 and 46°C for the Pen-Penultimate-Effect Model

Curve	r_3	r_5	r_7
1	2.0	10^4	0.3
2	10	10^4	2.0
3	100	10^4	2.0

TABLE 7. Reactivity Ratios for Copolymerization in the Temperature Range -78 to -18°C for the Complex Participation Model

Temperature (°C)		r_0	r_1	p_0	p_1	s_0	s_1	K
-78	a	0	0.1	0	0.5	10	10	0.1
	b	0	0.1	0	0.25	2.1	10	0.1
-45		0	0.1	0	6.6	2.6	10	0.1
-18		0	0.1	0	50	0.54	10	0.1

[a]Derived from direct measurements of copolymer composition.
[b]Fit to copolymer compositions derived from sequence distributions.

computer-based, patterned search procedure described previously [10] to derive "best estimates" of the reactivity ratios. We have taken $r_0 = 0$ and $p_0 = 0$ since there was no evidence for SS sequences in the copolymers. Copolymer compositions were available both from direct analysis (IR, NMR, and microanalysis), and from experimental sequence distributions using Eq. (3).

When matching the experimental copolymer/comonomer composition relationships, it was found that the shape of the calculated curves were particularly sensitive to the reactivity ratios p_1 and s_0. Best estimates of p_1 and s_0 were readily obtained at -78 and -45°C and are shown in Table 7. There appear to be some systematic discrepancies between the copolymer compositions measured directly and determined from sequence distributions at -78°C, resulting in different values of s_0. However, the overall trend with temperatures is similar.

In fitting the data at -18°C, no easily discernible minimum could be located on the hypersurface when all five parameters (reactivity ratios and equilibrium constant) were relaxed. Therefore, a value of p_1 at -18°C was predicted using an Arrhenius relationship and the

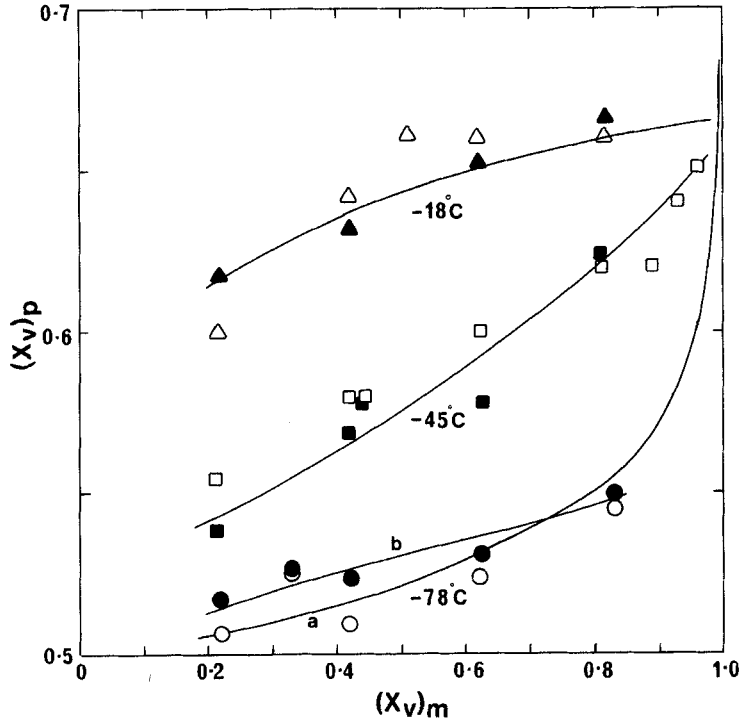

FIG. 5. Copolymer versus comonomer composition relationships calculated for the complex model at -78, -45, and -18°C from the reactivity ratios shown in Table 7. Experimental values: (○, ●) -78°C; (□, ■) -45°C; (△, ▲) -18°C. Open symbols: Measurements of copolymer composition. Closed symbols: Copolymer compositions calculated from experimental sequence distributions.

values of p_1 at -78 and -45°C. The best values of the other reactivity ratios were then determined in the usual way.

The copolymer/comonomer composition relationships for -78, -45, and -18°C are shown in Fig. 5. The curves are calculated from the reactivity ratios given in Table 7. Figure 6 shows the calculated (full lines) and experimental sequence distributions at -78°C and there is excellent agreement. Similarly, at -45 and -18°C there is good agreement between the calculated and experimental sequence distributions, as shown in Figs. 7 and 8.

Dilution Effects. A negligible dilution effect on sequence distributions is predicted at -78°C as shown in Fig. 6 and this is in accord with experiment. The calculated effects of a fourfold dilution

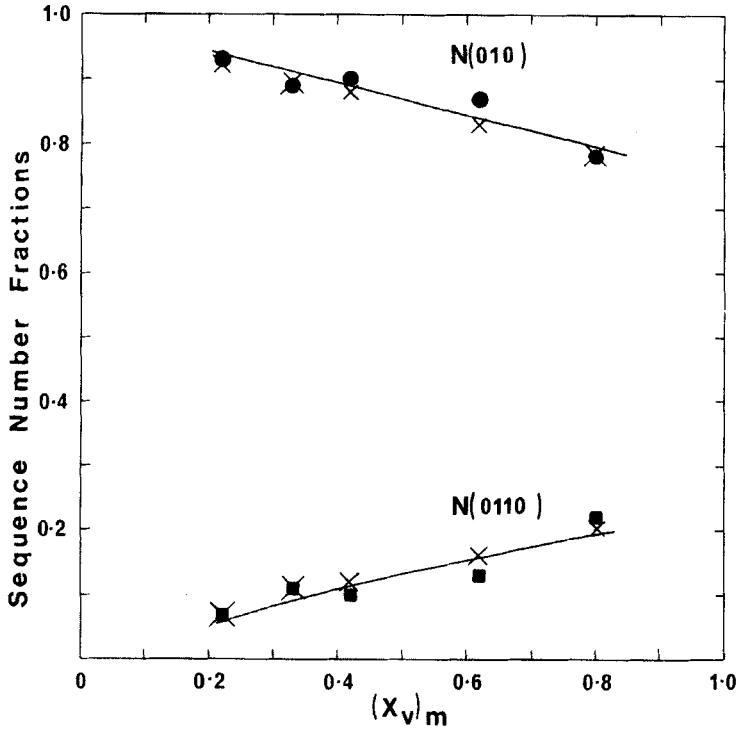

FIG. 6. Calculated (full lines) and experimental sequence distributions for the complex model at -78°C. Calculated: (—) undiluted; (×) fourfold dilution for the reactivity ratios (b) in Table 7. Experimental: (•) N(010) = number fraction of SVS sequences; (■) N(0110) = number fraction of SVVS sequences.

at -45 and -18°C are shown in Figs. 7 and 8, respectively, as functions of comonomer composition. There should be marked changes in sequence distribution at both temperatures. NMR measurements were made for equimolar comonomer mixtures at -78 and -18°C; these results are compared with predictions in Fig. 9. There is some uncertainty in the experimental value at -18°C for $[S] = 8$ mol/dm^3, since the smoothed copolymer versus comonomer composition data in Fig. 5 give a value for N(010) of ~0.2 at $(x_V)_m = 0.5$, which is in agreement with the predicted relationship in Fig. 9.

Conclusions. The complex-participation model can give a good fit to (1) copolymer compositions, (2) sequence distributions, and (3) dilution effects at -78, -45, and -18°C. This is not unreasonable since complex participation would be expected to increase with

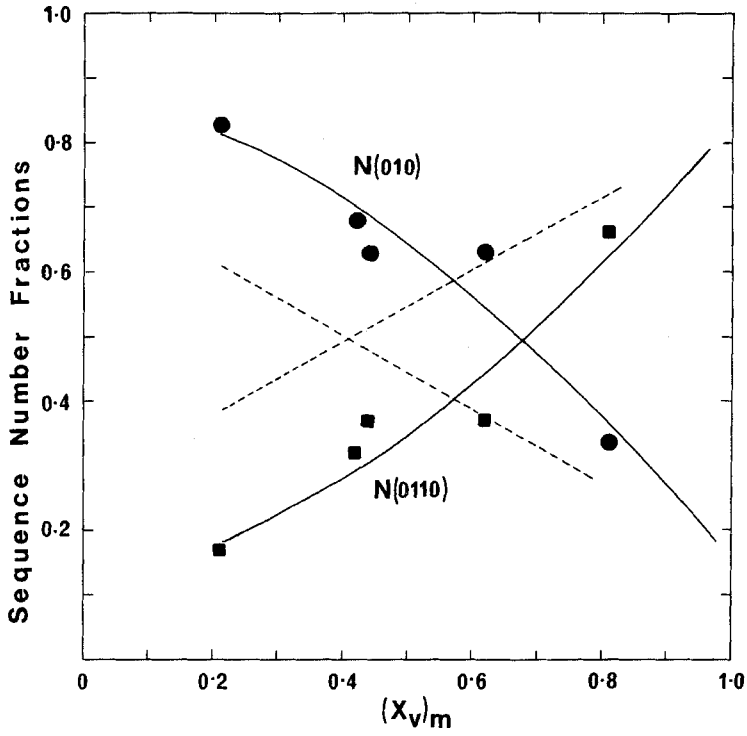

FIG. 7. Sequence distributions for the complex model at -45°C. Calculated: (—) undiluted; (- -) fourfold dilution for the reactivity ratios in Table 7. Experimental: (•) N(010); (▪) N(0110).

decreasing temperature when the concentration of the comonomer complex will increase and the reactivity of monomer molecules will decrease. At higher temperatures the reverse will apply and also depropagation can be expected to become of increasing importance. This may well be the reason for the decrease in s_0 at -18° C and the difficulty experienced in obtaining a clear minimum in the hypersurface, since $s_0 = k_{0\overline{10}}/k_{01}$ and would therefore reflect depropagation of the chain radical ~SVS*.

Interpretation of dilution effects on copolymer composition must be made with caution. Thus the computed curves show that dilution has only a small effect on the copolymer composition when (a) propagation proceeds almost exclusively by complex addition, or (b) complexes play a minor role in the copolymerization. However, when (c) the complex and free monomer are of comparable importance in the propagation mechanism, dilution gives an appreciable change in the

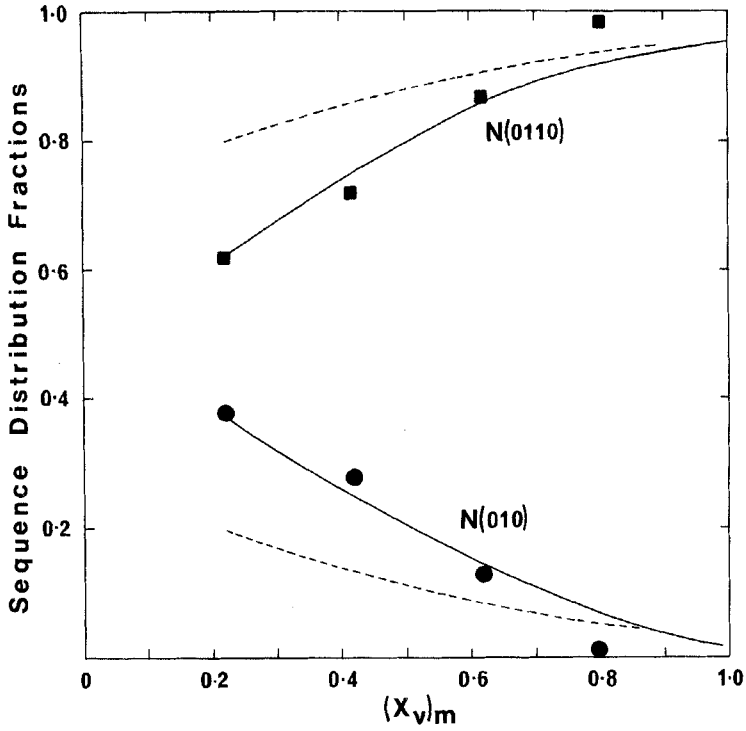

FIG. 8. Sequence distributions for the complex model at -18°C. Calculated: (—) undiluted; (- -) fourfold dilution for the reactivity ratios in Table 7. Experimental: (•) N(010); (■) N(0110).

copolymer/comonomer relationship. There is a noticeable similarity between the composition curves computed from the penultimate effect and the complex participation models, e.g., under conditions when reactions leading to the formation of ~0110~ sequences were important. This similarity between the models has been discussed elsewhere [11].

Depropagation Model

This model requires four reactivity ratios and three equilibrium constants, as well as the two monomer densities, for the copolymerization of vinyl chloride and sulfur dioxide. There is insufficient experimental data to allow a unique solution, but experimental measurements of the dependence of the copolymer compositions and sequence distributions on comonomer composition and temperature, the magnitude of the dilution effect, and the variation in

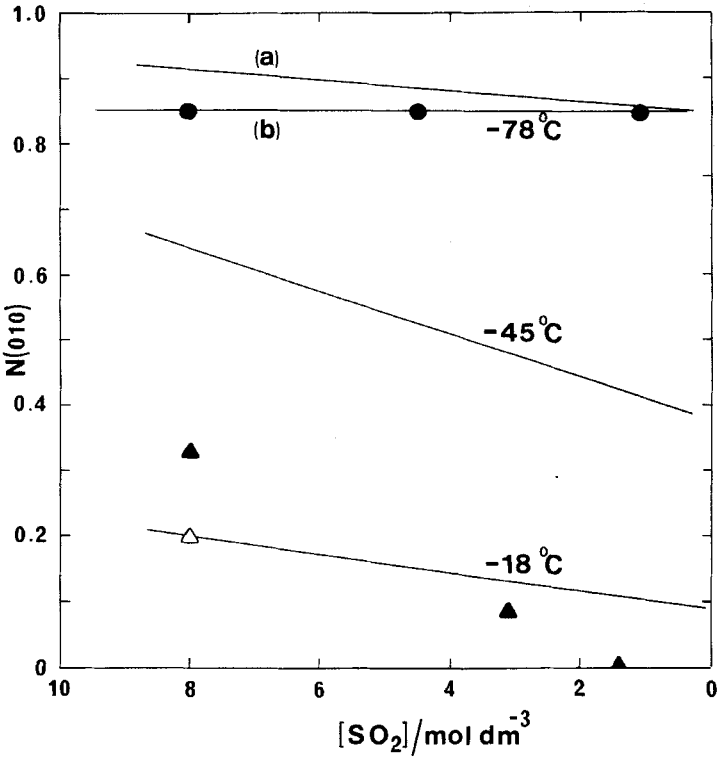

FIG. 9. Dilution dependence of the sequence distribution parameter N(010) for the complex model. Calculated: (—) for the reactivity ratios in Table 7. Experimental: (●) -78° C; (▲) -18° C; (△) value at -18° C interpolated from smoothed sequence versus composition relationship.

copolymerization rate and copolymer molecular weight enable reasonable values for the seven parameters to be derived.

We may make the following general observations.

r_1. This is equivalent to the Lewis-Mayo reactivity ratio and should be ≈0.05 at -78° C. It has been proposed that addition of S to alkyl radicals is a diffusion controlled reaction with almost zero activation energy, consequently the variation of r_1 with temperature should be due to the activation energy for homopropagation of V in liquid SO_2.

r_2. At sufficiently low temperatures, no penultimate effect on the addition of S to -V would be expected so that $r_2 = r_1$, but at higher temperatures -SV + S may be less favorable than -VV + S, and then $r_2 > r_1$.

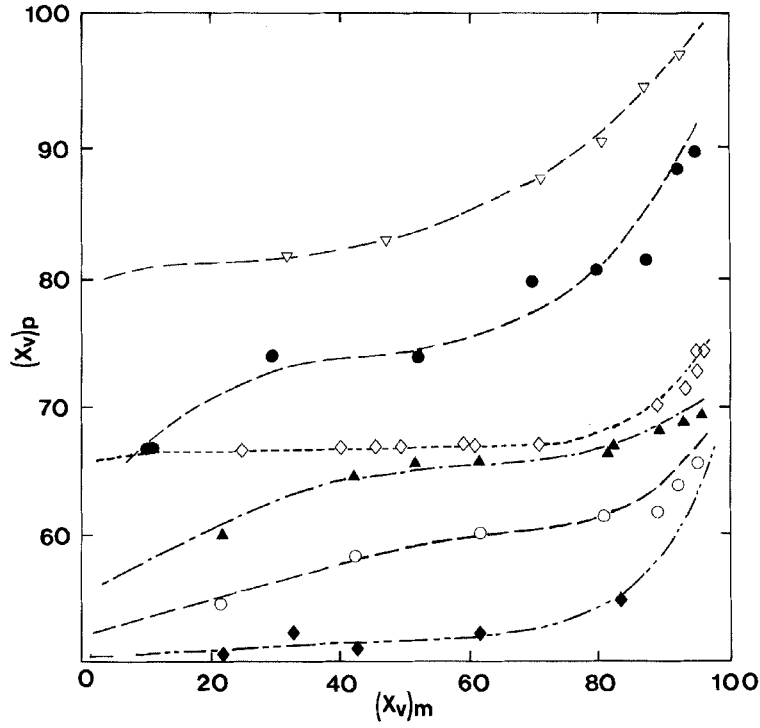

FIG. 10. Copolymer versus comonomer composition relationships calculated for the depropagation model in the temperature range -78 to +46° C from the reactivity ratios and equilibrium constants given in Table 8. The curves are the calculated relationships. Experimental values: (♦) -78° C; (○) -45° C; (▲) -18° C; (◇) 0° C; (●) 30° C; (▽) 46° C.

s_1 and s_2. Similarly, we would expect $s_1 = s_2$ at low temperatures, but a penultimate effect of S on the addition of S at higher temperatures would lead to $s_2 > s_1$. Also, with a high rate of addition of S to -V, both s_1 and s_2 should be greater than one. The effect of increasing temperature should be to decrease reactivity ratios greater than one (s_1 and s_2) and increase those less than one (r_1 and r_2) [15].

K_p. This equilibrium constant must decrease rapidly with increasing temperature to be $\ll 1$ at 0° C since only very small proportions of SVS sequences were incorporated in the polymer above 0° C.

K_V and K_T. Either or both of these equilibrium constants must

TABLE 8. Reactivity Ratios and Equilibrium Constants Used in the Temperature Range -78 to +46° C for Simulations of Copolymer Compositions and Sequence Distributions Using the Depropagation Model and Shown in Figs. 10 and 11. (D_1 and D_0 = densities of V and S, respectively.)

Temperature (° C)	r_1	r_2	s_1	s_2	K_p	K_V	K_T	D_1	D_0
-78	0.01	0.04	20	20	10	500	400	17.4	25.43
-45	0.01	0.04	10	11	0.1	120	100	16.45	24.13
-18	0.03	0.075	5	10	0.01	110	100	15.06	23.08
0	0.05	0.8	3	8	0.001	100	10	15.15	22.37
30	0.09	0.9	5	7	0.001	100	0.1	14.27	21.17
46	0.20	1.0	1	1	0.001	100	0.01	13.78	20.40

decrease with increasing temperature to account for the decreasing S content of the copolymer above 0° C.

The depropagation model reduces to the Lewis-Mayo model when K_p, K_V, and $K_T \gg 1$ and there are no penultimate unit effects on monomer addition, i.e., $r_1 = r_2$ and $s_1 = s_2$. This situation is approached at -78° C, but it is interesting that the best fit to the experimental data at -78° C, shown in Fig. 10, is given by $r_1 = 0.01$ and $r_2 = 0.04$, indicating that there is still a small penultimate unit effect on the addition of S to -V. The values of the equilibrium constants used in the computer simulations are given in Table 8.

Excellent agreement between simulated copolymer/comonomer composition relationships and experimental results were obtained at -45 and -18° C by greatly reducing K_p, slightly increasing r_1 and r_2 and reducing s_1 and s_2, as shown in Table 8 and Fig. 10.

At 0° C an excellent fit between simulation and experiment is obtained (Fig. 10). The chosen parameters allow for a rapidly decreasing equilibrium constant for the cross-propagation reaction -SV + S (K_p decreasing) and enhanced addition of V to both -V (causing r_1 and r_2 to increase) and to -S (causing s_1 and s_2 to decrease).

The fit of the simulations at 30 and 46° C shown in Fig. 10 are predominantly due to decreasing K_T, and further increasing r_1 and decreasing s_1 and s_2.

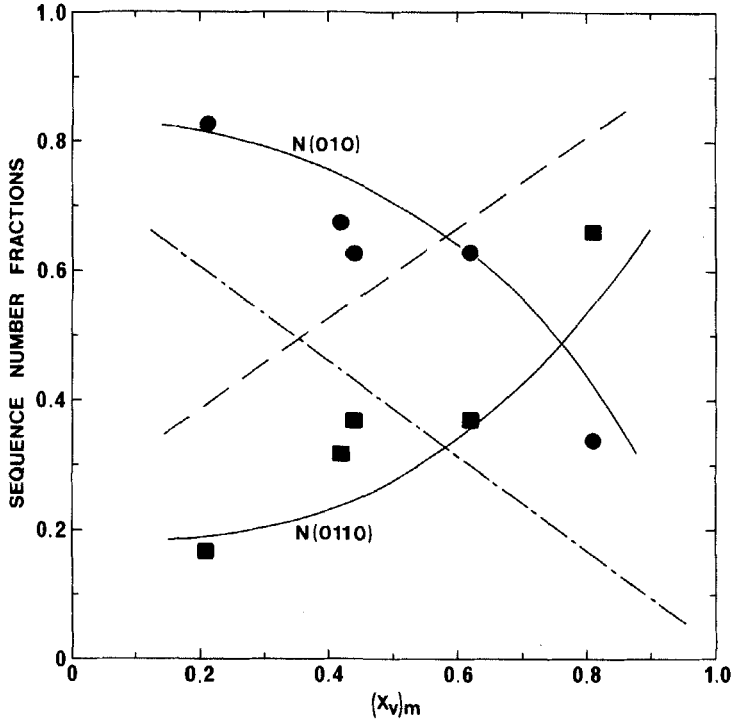

FIG. 11. Sequence distributions for the depropagation model at -45° C. Calculated: (—) undiluted; (- • -), (- -), fourfold dilution for N(010) and N(0110), respectively, for the parameters in Table 8. Experimental: (•) N(010); (▪) N(0110).

The sequence distributions in the copolymers are also readily obtained from the Monte-Carlo simulations of the copolymerization. Figure 11 shows the calculated variation of N(010) and N(0110) with comonomer composition for polymerization at -45° C using the reactivity ratios in Table 8. They are in quite reasonable agreement with the experimental values. The effect of dilution is also shown. The sequence distributions calculated for polymerization at -18° C are shown in Fig. 12 and compared with the experimental values; the agreement is again quite good.

The simulations also predict that dilution will cause $\bar{n}$ to increase substantially at 30° C, but only to a small extent at -18° C. The quantitative predictions for $(x_S)_m = 0.5$ are shown in Fig. 13, and are in adequate agreement with the experimental results if the experimental and calculated uncertainties are taken into account. In general, the

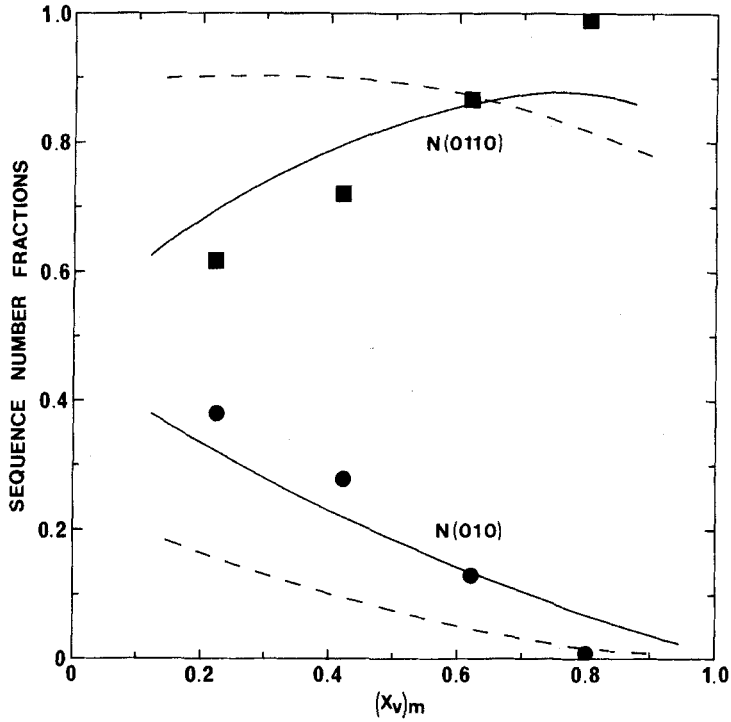

FIG. 12. Sequence distributions for the depropagation model at -18°C. Calculated: (—) undiluted; (- -) fourfold dilution for the parameters in Table 8. Experimental: (•) N(010), (▪) N(0110).

sequence distributions calculated from the Monte-Carlo simulation of the copolymerization show much greater fluctuations between repeated simulations than do the copolymer compositions. Therefore, much longer simulations are desirable, but the computer time increases proportionately.

The effect of progressive dilution at -18°C on the sequence distributions is shown in Fig. 14, and is in excellent agreement with the experimental results. Comparison of calculated and experimental dilution effects on sequence distributions for polymerizations above 0°C cannot be made because we have been unable to determine them experimentally.

The net rate of propagation, which will also affect the molecular weight, is markedly reduced with increasing temperature, except at high x_V, and although the temperature dependence of the termination

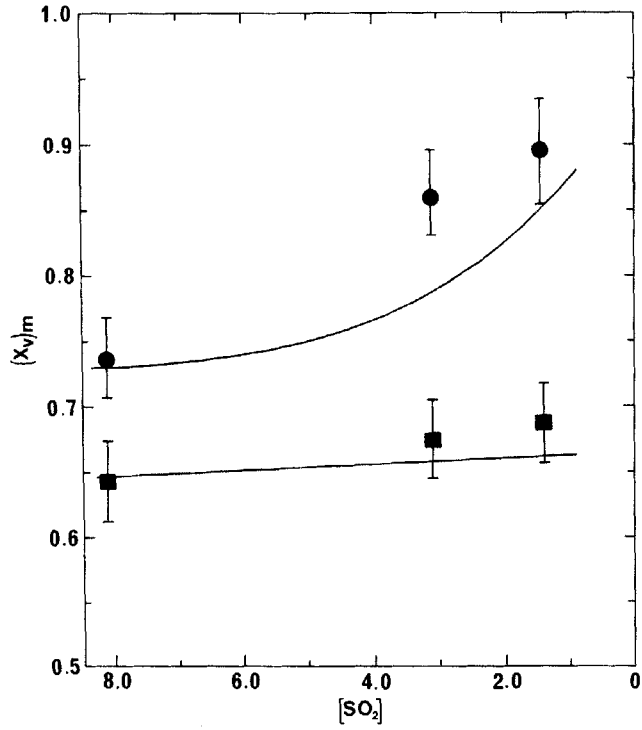

FIG. 13. Dilution dependence of the copolymer compositions at 30 and -18° C for the depropagation model. [V]/[S] = 1.0. Calculated: (—) for the reactivity ratios and equilibrium constants given in Table 8. Experimental values: (●) 30° C; (■) -18° C. Estimated uncertainties in experimental values are shown by error bars.

reactions will also affect copolymerization rate and molecular weight, this trend is in agreement with the experimental observations [1].

The reactivity ratios given in Table 8 are not a unique set, but they do show that the depropagation model can be used to predict the observed copolymer compositions over the whole temperature range from -78 to 46° C with reasonable accuracy. Other sets of reactivity ratios can be found in which the parameters also change systematically with temperature. In particular, we have shown that for $T_p \geq 0°C$, K_V decreasing more rapidly than K_T gives compositions in accord with experiment. The temperature dependence of K_T becomes important at the higher temperatures. Thus the copolymer composition data at 46° C can be adequately fitted by the following sets of parameters:

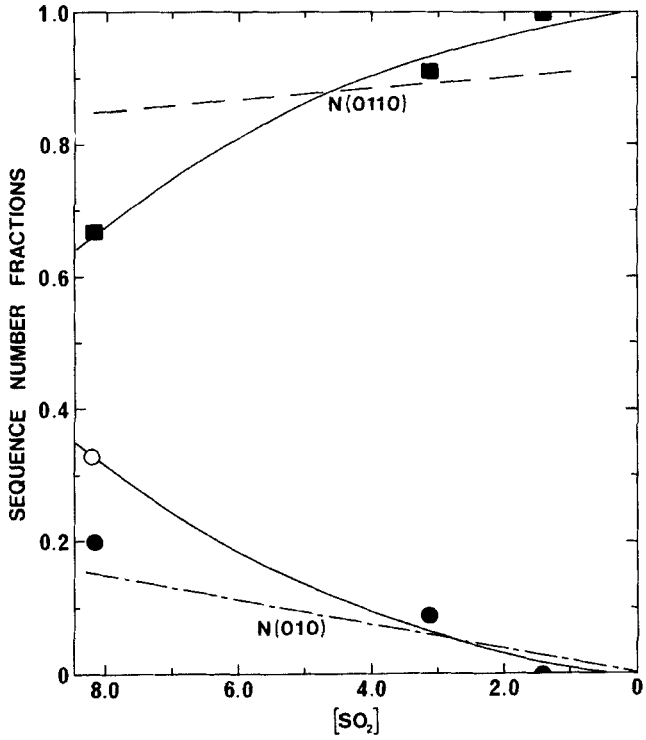

FIG. 14. Dilution dependence of the sequence number fractions N(010) and N(01110) for the depropagation model at -18° C. Calculated: (—) for the reactivity ratios and equilibrium constants given in Table 8. (●), (■): Experimental values; (○) derived from the smoothed curve through the experimental copolymer compositions using Eq. (3).

($r_1 = 2.0$, $r_2 = 5.0$, $s_1 = 1.0$, $s_2 = 1.0$, $K_p = 10^{-4}$, $K_V = 5 \times 10^{-3}$, $K_T = 1.0$) and ($r_1 = 0.2$, $r_2 = 0.8$, $s_1 = 3.0$, $s_2 = 5.0$, $K_p = 10^{-4}$, $K_V = 5 \times 10^{-3}$, $K_T = 0.6$).

Analysis of the sequence distributions obtained from the Monte-Carlo simulations using the various sets of parameters which provide acceptable representation of the composition data shows that experimentally determined distributions would be able to distinguish between some sets of parameters, at least for some copolymer compositions. For example, the two sets of parameters given above lead to distinguishable number fractions of 0110 sequences for the copolymers containing 60% of vinyl chloride, viz., 0.15 and 0.23.

CONCLUSIONS

Our previous paper [1] indicated that the copolymerization of vinyl chloride and sulfur dioxide could be divided into two regions of different behavior, viz., below and above 0°C. The suggestion was made that the mechanism of the copolymerization could be different in each region. The detailed analyses of the applicability of different possible mechanisms reported in this paper support this hypothesis.

Depropagation of the propagating triad -SVS below 0°C and of the triad -VVS or -VSV above 0°C has been shown to give an adequate description of the copolymer versus comonomer composition relationships from -78 to +46°C. The predicted effects of dilution on copolymer composition in increasing $\bar{n}$ substantially at 30°C, but only slightly at 0°C, are in agreement with our results.

It is important to recognize the difference between depropagation of the triad chain ends -SVS and -VVS. The former occurs more readily and the equilibrium constant, Kp, becomes so low by 0°C that SVS sequences are rare in the copolymer formed at or above 0°C. We have shown that the formation at 0°C of poly(vinyl chloride sulfone) with $\bar{n}$ = 2.0, and in particular with a great predominance of SVVS sequences, results from the complete depropagation of -SVS triad propagating radicals, whereas the depropagation of -VVS is insignificant. Above 0°C, we have found that the experimental results for copolymer compositions can be fitted readily with K_T or K_V decreasing rapidly. We have not found any need to invoke the "second-order" depropagation reaction proposed by Matsuda and Thoi [7].

The participation of comonomer complex in the copolymerization below 0°C cannot be ruled out, as stated by Matsuda and Thoi. Indeed, the copolymer/comonomer compositions and sequence distributions can be adequately explained at -78, -45, and -18°C by the complex model, although at -18°C the shallow minimum in the estimation of s_0 suggests involvement of depropagation.

Dilution effects observed between -78 and 0°C, when both copolymer compositions and sequence distributions were measured, can be accounted for quantitatively by either depropagation of -SVS triads or participation of comonomer complexes. It is probable that the complex is more important toward the lower end of this temperature range and depropagation of -SVS toward the upper end.

APPENDIX

Sequence Distributions

Copolymerization is a stochastic process and therefore the relative proportions of V_n sequences for different values of n can be calculated from probability theory.

The number fraction of sequences of 1 units of length n is defined by

$$N(n) = p(01^n0)/\sum_{n=1}^{\infty} p(01^n0) = p(01^n0)/p(10) \qquad (A\text{-}1)$$

The copolymer composition is defined by

$$\bar{n} = p(1)/p(0) \qquad \text{or} \qquad F_1 = p(1)/[p(1) + p(0)]$$

where F_1 is the mole fraction of units from monomer 1 in the copolymer.

The unconditional probabilities in Eq. (A-1) are related to conditional probabilities P_{JK} according to the Markovian order of the copolymerization mechanism and each P_{JK} can be related to appropriate reactivity ratios and the mole fractions f_0 and f_1 of the comonomers. The copolymer composition and sequence distribution may be derived by using statistical stationarity [16] or matrix algebra [17, 18] methods.

I. Pen-Penultimate Effect Model

The reaction scheme is shown in Table 2. A transition matrix of conditional probabilities is set up [19] and the corresponding secular determinant is solved to give values for the cofactors V_0 to V_7 corresponding to the relative proportions of the eight distinguishable triad sequences in an infinite chain, given by the decimal states in Table 2. The binary notation suggested by Price [17, 19] is used with S = 0 and V = 1. It follows that

$$p(0) = V_0 + V_2 + V_4 + V_6 \qquad (A\text{-}2)$$

$$p(1) = V_1 + V_3 + V_5 + V_7$$

The cofactors V_0 to V_7 are evaluated in terms of the conditional transition probabilities P_{JK} by expansion of the determinant [19]. The transition probabilities are expressed in terms of the rate constants for propagation and monomer concentrations using Bayes's rule.

The sequence distribution equations are derived as follows:

$$p(01^n0) = p(0111) \cdot P(111,1)^{n-3} \cdot P(111,0) \qquad (A\text{-}3)$$

but

$$p(0111) = p(011) \cdot P(011,1)$$

$$= p(01) \cdot P(01,1) \cdot P(011,1) \qquad \text{(A-4)}$$

Utilizing Eqs. (A-2), (A-3), and (A-4) and substituting the transition probabilities P_{JK} defined in Table 2, we obtain

$$N(n) = P(01,1) \cdot P_{37} \cdot P_{76} \cdot (P_{77})^{n-3}, \qquad \text{for } n \geq 3 \qquad \text{(A-5)}$$

and, for n = 2,

$$p(0110) = p(01) \cdot P(01,1) \cdot P(011,0)$$

hence

$$N(2) = P(01,1) \cdot P_{36} \qquad \text{(A-6)}$$

and for n = 1,

$$p(010) = p(01) \cdot P(01,0)$$

hence

$$N(1) = P(01,0) = 1 - P(01,1) \qquad \text{(A-7)}$$

P(01,1) must be evaluated in terms of the probabilities in Table 2. It is given by

$$P(01,1) = \frac{P_{53}(1 - P_{24}) + P_{24}(1 - P_{12})}{P_{53}(1 - P_{24}) + P_{24}(1 - P_{12}) + P_{12}(1 - P_{65}) + P_{65}(1 - P_{53})} \qquad \text{(A-8)}$$

For the copolymerization of vinyl chloride and sulfur dioxide,

$$r_0 = r_2 = r_4 = r_6 = 0$$

$$P_{00} = P_{24} = P_{40} = P_{64} = 0$$

$$P_{01} = P_{25} = P_{41} = P_{65} = 1$$

and the general relationships for p(1), p(0), and P(01,1) reduce to

$$p(1) = [P_{76}(1 + P_{53}) + P_{37}P_{53}]/P_{76} \quad \text{(A-9)}$$

$$p(0) = 1 \quad \text{(A-10)}$$

$$P(01,1) = P_{53} \quad \text{(A-11)}$$

Therefore,

$$N(1) = 1 - P_{53} = P_{52} \quad \text{(A-12)}$$

$$N(2) = P_{53}P_{36} \quad \text{(A-13)}$$

$$N(n) = P_{53}P_{37}P_{76}(P_{77})^{n-3}, \qquad \text{for } n > 2 \quad \text{(A-14)}$$

II. Penultimate Effect Model

Equating the state transition probabilities which differ only by a pen-penultimate effect gives

$$P_{00} = P_{40},\ P_{01} = P_{41},\ P_{12} = P_{52},\ P_{13} = P_{53},$$

$$P_{24} = P_{64},\ P_{25} = P_{65},\ P_{36} = P_{76},\ P_{37} = P_{77}$$

Then $r_0 = r_4$, $r_1 = r_5$, $r_2 = r_6$, $r_3 = r_7$, and for copolymerization of vinyl chloride and sulfur dioxide $r_0 = r_2 = 0$, $P_{00} = P_{24} = 0$, $P_{01} = P_{25} = 1$.

Equations (A-8) and (A12)-(A14) then reduce to

$$p(1) = 1 + P_{13}/P_{36} \quad \text{(A-15)}$$

$$N(1) = P_{12} \quad \text{(A-16)}$$

$$N(n) = P_{13}P_{36}(P_{37})^{n-2}, \qquad \text{for } n > 1 \quad \text{(A-17)}$$

III. Terminal (Lewis-Mayo) Model

This is derived from II by equating the state transition probabilities which differ only by a penultimate effect:

$$P_{00} = P_{24},\ P_{01} = P_{25},\ P_{12} = P_{36},\ P_{13} = P_{37}$$

Then $r_0 = r_2$ and $r_1 = r_3$, and for copolymerization of vinyl chloride and sulfur dioxide $r_0 = 0$, $P_{00} = 0$ and $P_{01} = 1$.

Equations (A-15)-(A17) reduce to

$$p(1) = 1 + P_{13}/P_{12} \tag{A-18}$$

$$N(1) = P_{12} \tag{A-19}$$

and

$$N(n) = P_{12}(P_{13})^{n-1}, \qquad \text{for } n > 1 \tag{A-20}$$

ACKNOWLEDGMENTS

The authors wish to thank the Australian Research Grants Committee and the Australian Institute of Nuclear Science and Engineering for supporting this research. They are grateful to Mr M. Williams, Mr M. Ash, Mr D. Van Bruggen, and Miss J. Bull for assistance with the calculations and to Mr P. W. O'Sullivan and Dr R. Farmer for advice on the computer programs.

REFERENCES

[1] R. E. Cais and J. H. O'Donnell, J. Macromol. Sci.–Chem., A17, 1407 (1982).
[2] C. Schneider, J. Denaxas, and D. Hummel, J. Polym. Sci., Part C, 16, 2203 (1967).
[3] H. Suzuki, M. Ito, and Z. Kuri, Kogyo Kagaku Zasshi, 71, 764 (1968).
[4] W. G. Barb, Proc. R. Soc. (London), A212, 66 (1952).
[5] R. E. Cais and J. H. O'Donnell, Eur. Polym. J., 11, 749 (1975).
[6] R. E. Cais and J. H. O'Donnell, J. Polym. Sci., Polym. Lett. Ed., 15, 659 (1977).
[7] M. Matsuda and H. H. Thoi, J. Macromol. Sci.–Chem., A11, 1423 (1977).
[8] R. E. Cais and J. H. O'Donnell, Macromolecules, 9, 279 (1976).
[9] R. E. Cais and J. H. O'Donnell, J. Macromol. Sci.–Chem., A10, 769 (1976).
[10] R. E. Cais, R. G. Farmer, D. J. Hill, and J. H. O'Donnell, Macromolecules, 12, 835 (1979).
[11] J. A. Seiner and M. Litt, Ibid., 4, 308 (1971).
[12] J. A. Howell, M. Izu, and K. F. O'Driscoll, J. Polym. Sci., Part A-1, 8, 699 (1970).

[13] J. I. Lauritzen, E. A. DiMarzio, and E. Passaglia, J. Chem. Phys., 45, 4444 (1966).
[14] M. Izu and K. F. O'Driscoll, J. Polym. Sci., Part A-1, 8, 1675 (1970).
[15] K. F. O'Driscoll, J. Macromol. Sci.–Chem., A3, 307 (1969).
[16] C. W. Pyun, J. Polym. Sci., Part A-2, 8, 1111 (1970).
[17] F. P. Price, J. Chem. Phys., 36, 209 (1962).
[18] L. Peller, Ibid., 43, 2355 (1965).
[19] F. P. Price, in Markov Chains and Monte Carlo Calculations in Polymer Science (G. G. Lowry, ed.), Dekker, New York, 1970, p. 197.

Accepted by editor May 12, 1981
Received for publication June 2, 1981